

Available online at www.synsint.com

Synthesis and Sintering

ISSN 2564-0186 (Print), ISSN 2564-0194 (Online)



Research article

Role of Ti_3AlC_2 MAX phase on characteristics of in-situ synthesized TiAl intermetallics. Part IV: mechanical properties



Maryam Akhlaghi ^a, Esmail Salahi ^{b,*}, Seyed Ali Tayebifard ^a, Gert Schmidt ^c

^a Semiconductors Department, Materials and Energy Research Center (MERC), Karaj, Iran

^b Ceramics Department, Materials and Energy Research Center (MERC), Karaj, Iran

^c Faculty of Mechanical, Process and Energy Engineering, TU Bergakademie, Freiberg, Germany

ABSTRACT

In this study, the 4th part of a series of publications on the sintering and characterization of TiAl- Ti_3AlC_2 composite materials, the mechanical properties were measured and discussed. For this purpose, different contents of synthesized Ti_3AlC_2 reinforcement (10, 15, 20, 25, and 30 wt%) were added to metallic Ti and Al powders, then ball-milled and manufactured by spark plasma sintering (SPS) for 420 s at 900 °C under 40 MPa. Flexural strength, fracture toughness and Vickers hardness were measured by 3-point technique, SENB method, and indentation technique, respectively. Increasing the Ti_3AlC_2 content resulted in improvement of the mechanical properties, so that TiAl-25 wt% Ti_3AlC_2 composite showed the best flexural strength and Vickers hardness (270 MPa and 4.11 GPa, respectively). Increasing amount of Ti_3AlC_2 additive had no significant effect on fracture toughness. Densification improvement, in-situ formation of Ti_2AlC , and limitation of grain growth were recognized as the reasons of mechanical properties enhancement. In contrast, further addition of Ti_3AlC_2 (30 wt%) decreased the mechanical properties due to the reduction of density and formation of more Ti_2AlC agglomerates in grain boundaries.

© 2022 The Authors. Published by Synsint Research Group.

KEYWORDS

SPS
TiAl- Ti_3AlC_2
Flexural strength
Hardness
Fracture toughness



1. Introduction

Privileged features of titanium aluminides like high creep and oxidation resistance, good corrosion properties, high melting point, and low density has made them potential candidates for using in different high-temperature applications and aircraft engines [1–4]. However, mechanical characteristics of TiAl-based materials have been influenced by microstructure, which can vary with changing in fabrication parameters and composition. Although adding the hard and stiff particles promotes the strength, it leads to a decrease in ductility [5–8]. Hence, development of the intermetallic matrix composites (IMCs) have gained researchers attention to improve the low temperatures ductility and to attain the suitable combination of creep resistance and high-temperature strength. Reinforcing phases like

Ti_2AlC , TiB_2 , Al_2O_3 , and Ti_5Si_3 have been used as the stable and desired components in TiAl-based composites [9–11]. Several researches show that the mechanical efficiency of such composite materials can be greatly improved by reduction of the reinforcement particle size. The in-situ method of combustion synthesis and hot press consolidation were utilized to manufacture TiAl-based composites reinforced with nano- Ti_5Si_3 and nano- TiB_2 . Ultimate compression strength improvement and reduction of work-hardening capacity (H_c) of the TiAl matrix occur when the content of TiB_2 increases, owing to the formation of network structure and the refined microstructure of the matrix. Also, increase in the Ti_5Si_3 amount in TiAl-based composite first enhances the ultimate compression strength and fracture strain and then decreases them [12]. Fabrication of TiAl-based composites reinforced with MAX phases resulting in obtain the competency of

* Corresponding author. E-mail address: e-salahi@merc.ac.ir (E. Salahi)

Received 24 January 2022; Received in revised form 29 June 2022; Accepted 29 June 2022.

Peer review under responsibility of Synsint Research Group. This is an open access article under the CC BY license (<https://creativecommons.org/licenses/by/4.0/>).
<https://doi.org/10.53063/synsint.2022.22103>

ceramics and metals, simultaneously [13]. MAX phases with hexagonal lamellar structure showing unique physical, chemical, mechanical, and electrical properties belongs to the relatively new group of materials [14–17]. It is reported that the uniformly distribution of Ti_2AlC grains in TiAl matrix through in-situ reactive hot pressing of a mixture of Al, Ti and TiC leads to the improvement of bending strength and fracture toughness [18]. According to the layered structure and dispersion effect of hard particles, only small quantities addition of Ti_2AlC phase in TiAl-based material, manufactured by reactive spark plasma sintering method using Ti, Al, and TiC powders, leads to the enhancement of both bending strength and toughness [19]. It is reported that $Ti_2AlC/TiAl$ composite with ultrafine microstructure can be prepared by spark plasma sintering of Ti, Al, and CNTS mixed by mechanical alloying method. 6.12 GPa and 2058 MPa were measured for hardness and the compressive yield strength of the SPSed samples at 950 °C, respectively. The increasing of processing temperature up to 1150 °C resulted in reduced mechanical properties due to the grain growth [20]. The flexural strength of TiAl/ Ti_2AlC composites, fabricated by spark plasma sintering of powder mixture of TiC, Al, and Ti can attain 900 MPa [19].

In addition to introduction of secondary phases in TiAl matrix, selecting the appropriate processing technique can be utilized to overcome these problems [9–11]. Compared to other conventional methods, spark plasma sintering route is one of the recently developed methods that has several superiorities like high processing speed, lower sintering temperatures, reproducibility leading to achieve refined and homogeneous microstructures, [21–24].

In present study, TiAl-based composite materials reinforced with 10, 15, 20, 25, and 30 wt% Ti_3AlC_2 MAX phase were sintered by SPS method at temperature of 900 °C under a load of 40 MPa for dwell time of 7 min. This paper is 4th section of series of papers that will study the mechanical characteristics of as-prepared composite samples. The densification behavior, phase evolution, and microstructure development were investigated in pervious 3 papers of these series [25–27].

2. Experimental procedure

Commercial Al and Ti powders in equal molar proportion were used as the raw materials to produce the TiAl matrix via chemical reaction utilizing SPS method. The self-propagating high-temperature synthesis (SHS) of the mechanically-activated powder mixtures of elemental Al, Ti and graphite was used to synthesis of the Ti_3AlC_2 MAX phase (details are in Ref. [28]). Also, 15 wt% TiC was synthesized as the impurity phase during the preparation of Ti_3AlC_2 MAX phase, in other words, the purity of 85 wt% was obtained for prepared Ti_3AlC_2 . Various contents of Ti_3AlC_2 (10, 15, 20, 25, and 30 wt%) as the reinforcement phase were added in the TiAl matrix composites. After weighting the powders, the mixed Al, Ti and Ti_3AlC_2 powders were ball-milled at 300 rpm for 60 min. The attained powder mixtures individually filled into the graphite molds, covered by flexible graphite sheet to prevent chemical reaction between the mold and powder mixture. After placing the mold in the SPS device (model: 20T-10), an initial load of ~8 MPa and a preliminary vacuum of 12–15 Pa was applied (details are in [25]). Finally, the synthesis and densification process were carried out through spark plasma sintering technique for 7 min under a pressure of 40 MPa at 900 °C. In order to remove graphite foil from the surfaces of as-sintered samples, the spark plasma sintered

samples were ground using diamond grinding plate. The rods were prepared in dimensions of $3 \times 4 \times 25$ mm³ (as shown in Fig. 1) for flexural strength test utilizing wire cut device (Charmilles Robofill 310 wire EDM) by a wire with thickness of 0.25 mm. The cut sections of rods and some sectioned as-sintered composite samples were polished using abrasive paper made of SiC from 100 to 5000 mesh and diamond lapping paste to prepare for the flexural strength and Vickers hardness tests, respectively. Flexural strength of as-sintered samples was determined by three-point technique using the 2-cm length of gauge with a crosshead speed of 0.5 mm/min on the cut rods at ambient temperature (ASTM C-1161- 02C). Measurement of fracture toughness of as-sintered composite samples was done through single edge notched beam (SENB) technique on $3 \times 4 \times 25$ mm³ rods. Before testing, a sharp notch to a depth of 0.4 of the sample width was cut in the center of the each sample. The notched rods samples were tested in a 3-point bending test device. A constant crosshead rate of 0.5 mm/min and a fixed gauge length of 2 cm were utilized at ambient temperature. Values of fracture toughness were calculated using the following equations:

$$K_{IC} = \frac{3PLa^{\frac{1}{2}}}{2BW^{\frac{3}{2}}} \times Y \quad (1)$$

where P, L, a, W, B, and Y are the maximum load applied on the rods, gauge length, depth of notch, sample width, rod thickness, and geometric constants, respectively.

Indentation method was used to evaluate Vickers hardness of as-sintered composites by applying a load of 2 kg using Vickers diamond pyramid. Field emission scanning electron microscopy (Mira3, TESCAN) was used for investigation of indentation trace and following the crack paths.

3. Results and discussion

In present part, the mechanical properties of TiAl- Ti_3AlC_2 composite materials are studied. This part is 4th section of a series that three sections of them have recently been published. The sintering and densification behavior were discussed in the 1st section of these series [25], the phase characterization was studied in the 2nd section of these series [26], and the microstructure investigation was reported in the 3rd section of these series [27]. Table 1 presents the results of the measured

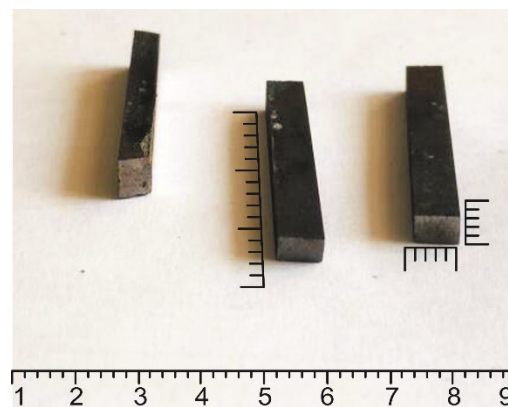


Fig. 1. Wire cut rod samples for flexural strength test.

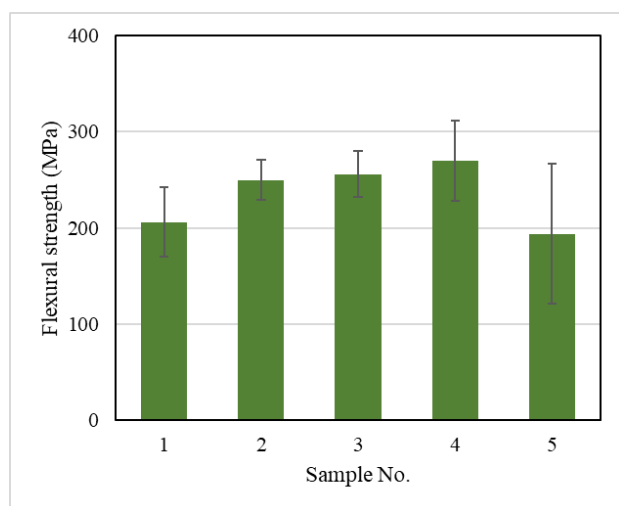
Table 1. Mechanical properties of as-sintered composite samples.

Sample no.	Bending strength (MPa)	Vickers hardness (GPa)	Fracture toughness ($\text{MPa}\cdot\text{m}^{1/2}$)
1	206 ± 36	3.61 ± 0.81	10.89 ± 0.74
2	250 ± 21	3.65 ± 0.73	11.75 ± 0.52
3	256 ± 24	3.68 ± 0.42	11.11 ± 0.25
4	270 ± 42	4.11 ± 0.55	11.21 ± 0.33
5	194 ± 73	2.91 ± 0.31	9.01 ± 0.95

mechanical properties of five as-sintered samples. As it can be seen in Table 1, the mechanical properties of the sample 4 are most desired among other samples, while sample 5 shows the weakest mechanical characteristics.

3.1. Bending strength

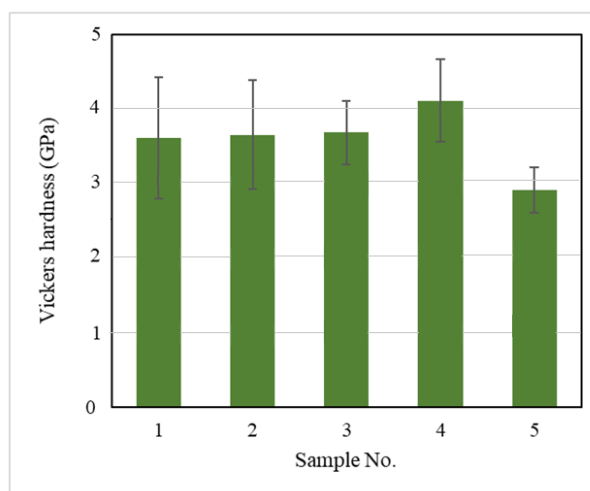
The measured flexural strength of as-sintered samples, tested in ambient temperature, is demonstrated in Fig. 2. The ability of a material to withstand deformation when applying an external pressure is known as the flexural strength. As it can be seen in Fig. 2, flexural strength of as-prepared samples increases with increasing Ti_3AlC_2 content up to 25 wt%, but further amount of Ti_3AlC_2 (30 wt%) leads to degradation of this property, so that the flexural strength of sample 5 was estimated 194 ± 73 MPa. It is worthy to mention that several items like size of grains, additive, as well as defects and relative density can affect value of flexural strength. The highest flexural strength of samples belongs to sample 4 (270 MPa). The grain size is the first factor affecting flexural strength of these samples. As it was shown in previous research [27], increasing in Ti_3AlC_2 content up to 25 wt% has led to microstructure refinement and limitation of grain growth. Therefore, sample 4 has the highest strength due to its fine-grained microstructure. This observation displays the significance of Ti_3AlC_2 content on densification, microstructure development, and improvement of flexural strength. When Ti_3AlC_2 content reaches to 30 wt%, existence phases become more continuous, leading to a

**Fig. 2.** Flexural strength of the as-sintered TiAl-based samples.

reduction in the grain boundary and thus a decrease in flexural strength. According to the reported relative density of 92.8% for sample 4 (see Ref. [25]) that is higher than that of other samples, higher flexural strength of this sample is logical. The relative density of 90.12% is reported for sample 5 containing 30 wt% Ti_3AlC_2 , which is the lowest value obtained for this quantity. Thus, degradation of relative density in sample 5 is another reason to reduction of flexural strength. Also, increasing the amount of Ti_3AlC_2 phase causes the more of Ti_2AlC phase formation at the grain boundaries of matrix, which not only prevents the growth of grains, but also increases the strength of grain boundaries. In contrast, increasing the additive content up to 30 wt% resulted in further agglomeration of this phase, increased defects and porosity, compared to samples containing lower content of reinforcement. It should be mentioned that the attained flexural strength for as-sintered samples is lower than that of matrix (360 MPa) [29] and reinforcement (375 MPa) [30] that can be due to not reaching full density.

3.2. Vickers hardness

Fig. 3 shows the Vickers hardness values of as-SPSed samples. As it can be seen in Table 1 and Fig. 3, Vickers hardness is improved from 3.61 to 4.11 GPa as the amount of Ti_3AlC_2 increased from 10 to 25 wt% in TiAl, but further addition of this MAX phase has the negative influence on this feature, so that with a hardness reduction of about 30% compared to the sample 5, the Vickers hardness of this sample reached 2.9 GPa. Hardness is known as a mechanical characteristic of a material demonstrating its resistance to localized permanent plastic deformation when applying the load, which is typically performed by the indentation technique. It is worth noting that Vickers hardness of materials with low relative density is lower than that of near fully dense ones due to the less resistance of porosities and pores against applied external load. As it was mentioned before, addition of Ti_3AlC_2 inhibits grows of matrix grains leading to refined microstructure and improved Vickers hardness. Further formation of Ti_2AlC , as a result of increasing amounts of Ti_3AlC_2 , with higher intrinsic hardness (4.5 GPa) [31] than that of Ti_3AlC_2 phase (2.7 GPa) [32], resulted in hardening the as-sintered samples. Microstructure

**Fig. 3.** Vickers hardness of the as-sintered TiAl-based samples.

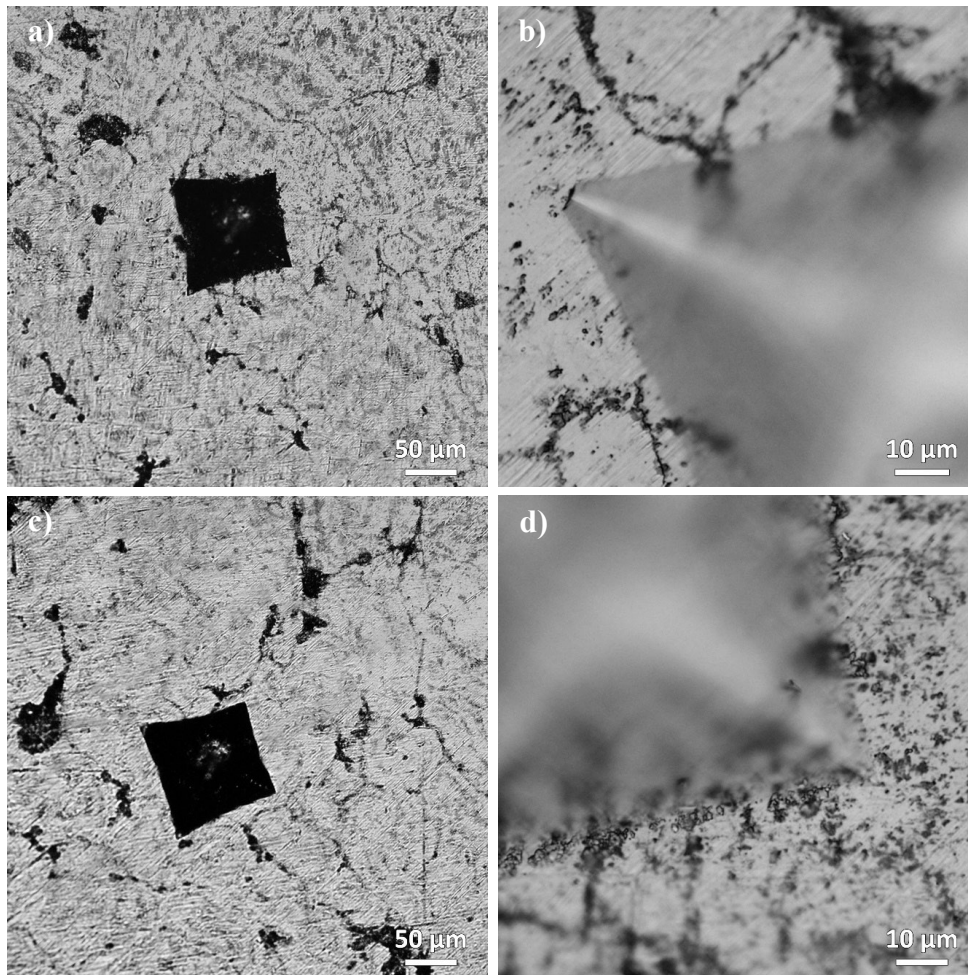


Fig. 4. Optical microscopy images of the Vickers indenter's impression on the polished surfaces of a, b) sample 2 and c, d) sample 4.

refinement is another reason for hardness improvement that carried out by increasing the reinforcement content. It seems that further addition of Ti_3AlC_2 in the microstructure of TiAl causes more agglomeration of these particles at the grain boundaries, which leads to the confinement of porosity and thus the reduction of hardness. Therefore, the hardness degradation in sample 5 is due to the lower resistance of agglomerates and porosities to plastic deformation when the load is applied.

Fig. 4 shows the optical microscopy images of the Vickers indenter's impression on the polished section of the samples.

3.3. Fracture toughness

Fig. 5 displays the fracture toughness values of as-SPSed samples. Compared to hardness and strength, the trend of toughness changes seems to be slightly different. Fig. 5 shows that the sample 2 has the highest fracture toughness ($11.85 \text{ MPa}\cdot\text{m}^{1/2}$) among the other sintered samples. Such fracture toughness is significantly higher in comparison in the values reported for many ceramic-based composites [33–36].

It is worthy to note, given the calculated standard deviation for samples 1 to 4 (containing 10 to 25 wt% Ti_3AlC_2), the difference in obtained fracture toughness does not seem to be very significant. Increasing the amount of Ti_3AlC_2 up to 30% reduces the fracture toughness by about 20%, so that the composite with fracture toughness of $9 \text{ MPa}\cdot\text{m}^{1/2}$ was

manufactured. Presence of porosities entrapped in microstructure causes decrease the toughness of sample 5.

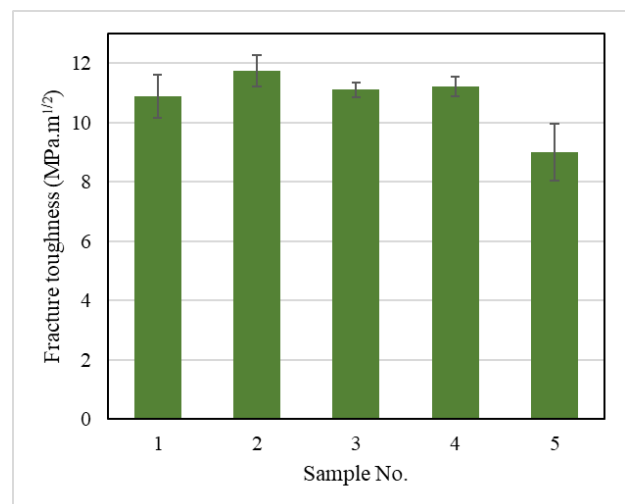


Fig. 5. Fracture toughness of the as-sintered TiAl-based samples.

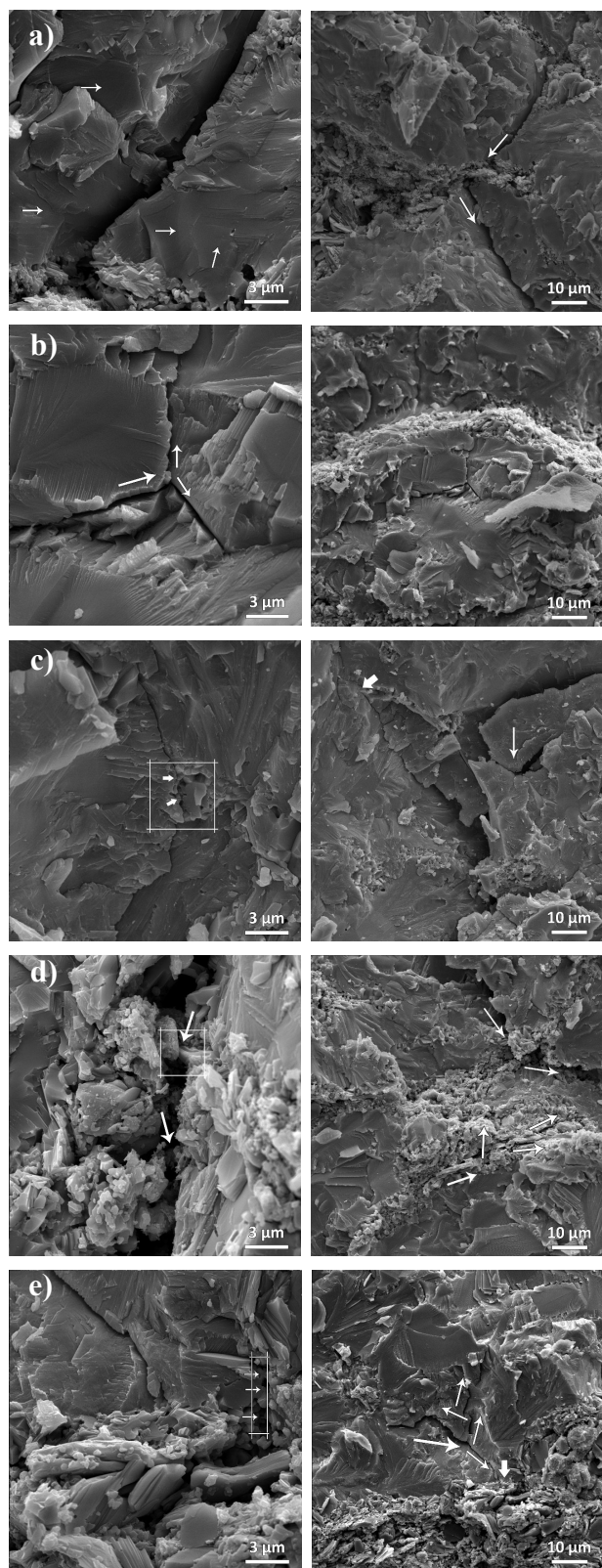


Fig. 6. SE-FESEM fractographs of a) sample 1, b) sample 2, c) sample 3, d) sample 4, and e) sample 5 tested by SENB method.

Fig. 6 exhibits the FESEM images of fractured surfaces of as-sintered samples during the SENB test and created cracks. Interaction of cracks with reinforcement phase like crack deflection, crack bridging and crack branching can be seen in Fig. 6. The layered structure of MAX phases with high aspect ratio can observe crack energy and enhance the fracture toughness.

4. Conclusions

Effect of different contents of Ti_3AlC_2 reinforcement (10, 15, 20, 25, and 30 wt%) on the mechanical properties of spark plasma sintered TiAl matrix composites was studied. SPS method was employed to densify the composite samples at 900 °C for 420 s under 40 MPa utilizing the ball-milled previously-synthesized Ti_3AlC_2 MAX phase with elemental Ti and Al powders. The mechanical properties of as-sintered samples (fracture toughness, Vickers hardness and flexural strength) were assessed. Increasing the reinforcement content up to 25 wt% led to enhancement of Vickers hardness and flexural strength of as-sintered samples, but it has no remarkable effect on the fracture toughness. Further increasing the Ti_3AlC_2 decrease the mechanical properties, according to the formation of more porosities in the microstructure and more agglomeration of Ti_3AlC_2 .

CRedit authorship contribution statement

Maryam Akhlaghi: Investigation, Data curation, Writing – original draft, Visualization.

Esmail Salahi: Project administration, Supervision, Methodology.

Seyed Ali Tayebifard: Conceptualization, Funding acquisition, Validation.

Gert Schmidt: Writing – review & editing.

Data availability

The data underlying this article will be shared on reasonable request to the corresponding author.

Declaration of competing interest

The authors declare no competing interests.

Funding and acknowledgment

The content of this article is based on the PhD thesis of the first author. The authors would like to express their gratitude to the Materials and Energy Research Center for its support of this research project under grant number 481394051. Additionally, the invaluable assistance of Dr. Behzad Nayebi in result analysis and Mrs. Masoumeh Enayati and Mrs. Nadi Shojaei in conducting the experiments is sincerely appreciated.

References

- [1] H.P. Lim, W.Y.H. Liew, G.J.H. Melvin, Z.-T. Jiang, A Short Review on the Phase Structures, Oxidation Kinetics, and Mechanical Properties of Complex Ti-Al Alloys, *Materials* (Basel). 14 (2021) 1677. <https://doi.org/10.3390/ma14071677>.
- [2] H. Huang, H. Ding, X. Xu, R. Chen, J. Guo, H. Fu, Phase transformation and microstructure evolution of a beta-solidified gamma-TiAl alloy, *J. Alloys Compd.* 860 (2021) 158082. <https://doi.org/10.1016/j.jallcom.2020.158082>.
- [3] Y. Jiang, Y. He, H. Gao, Recent progress in porous intermetallics: Synthesis mechanism, pore structure, and material properties, *J. Mater. Sci. Technol.* 74 (2021) 89–104. <https://doi.org/10.1016/j.jmst.2020.10.007>.

- [4] Z. Trzaska, G. Bonnefont, G. Fantozzi, J.-P. Monchoux, Comparison of densification kinetics of a TiAl powder by spark plasma sintering and hot pressing, *Acta Mater.* 135 (2017) 1–13. <https://doi.org/10.1016/j.actamat.2017.06.004>.
- [5] G.H. Cao, A.M. Russell, C.-G. Oertel, W. Skrotzki, Microstructural evolution of TiAl-based alloys deformed by high-pressure torsion, *Acta Mater.* 98 (2015) 103–112. <https://doi.org/10.1016/j.actamat.2015.07.012>.
- [6] C.Y. Teng, N. Zhou, Y. Wang, D.S. Xu, A. Du, et al., Phase-field simulation of twin boundary fractions in fully lamellar TiAl alloys, *Acta Mater.* 60 (2012) 6372–6381. <https://doi.org/10.1016/j.actamat.2012.08.016>.
- [7] J. Shen, L. Hu, L. Zhang, W. Liu, A. Fang, Y. Sun, Synthesis of TiAl/Nb composites with concurrently enhanced strength and plasticity by powder metallurgy, *Mater. Sci. Eng. A.* 795 (2020) 139997. <https://doi.org/10.1016/j.msea.2020.139997>.
- [8] Y. Garip, Investigation of isothermal oxidation performance of TiAl alloys sintered by different processing methods, *Intermetallics.* 127 (2020) 106985. <https://doi.org/10.1016/j.intermet.2020.106985>.
- [9] L. Xiang, F. Wang, J. Zhu, X. Wang, Mechanical properties and microstructure of Al₂O₃/TiAl in situ composites doped with Cr₂O₃, *Mater. Sci. Eng. A.* 528 (2011) 3337–3341. <https://doi.org/10.1016/j.msea.2011.01.006>.
- [10] H.P. Qu, P. Li, S.Q. Zhang, A. Li, H.M. Wang, The effects of heat treatment on the microstructure and mechanical property of laser melting deposition γ -TiAl intermetallic alloys, *Mater. Des.* 31 (2010) 2201–2210. <https://doi.org/10.1016/j.matdes.2009.10.045>.
- [11] H. Clemens, A. Bartels, S. Bystrzanowski, H. Chladil, H. Leitner, et al., Grain refinement in γ -TiAl-based alloys by solid state phase transformations, *Intermetallics.* 14 (2006) 1380–1385. <https://doi.org/10.1016/j.intermet.2005.11.015>.
- [12] S. Shu, B. Xing, F. Qiu, S. Jin, Q. Jiang, Comparative study of the compression properties of TiAl matrix composites reinforced with nano-TiB₂ and nano-Ti₅Si₃ particles, *Mater. Sci. Eng. A.* 560 (2013) 596–600. <https://doi.org/10.1016/j.msea.2012.10.001>.
- [13] D. Zhu, L. Liu, D. Dong, X. Wang, Y. Liu, et al., Microstructure and compression behavior of in-situ synthesized Ti₂AlC reinforced Ti-48Al-2Cr alloy with carbon nanotubes addition, *J. Alloys Compd.* 862 (2021) 158646. <https://doi.org/10.1016/j.jallcom.2021.158646>.
- [14] S. Haji Amiri, M. Ghassemi Kakroudi, T. Rabizadeh, M. Shahedi Asl, Characterization of hot-pressed Ti₃SiC₂-SiC composites, *Int. J. Refract. Met. Hard Mater.* 90 (2020) 105232. <https://doi.org/10.1016/j.ijrmhm.2020.105232>.
- [15] J. Lyu, E.B. Kashkarov, N. Travitzky, M.S. Syrtanov, A.M. Lider, Sintering of MAX-phase materials by spark plasma and other methods, *J. Mater. Sci.* 56 (2021) 1980–2015. <https://doi.org/10.1007/s10853-020-05359-y>.
- [16] S.H. Amiri, M.G. Kakroudi, N.P. Vafa, M.S. Asl, Synthesis and Sintering of Ti₃SiC₂-SiC Composites through Reactive Hot-Pressing of TiC and Si Precursors, *Silicon.* 14 (2022) 4227–4235. <https://doi.org/10.1007/s12633-021-01207-z>.
- [17] S. Haji Amiri, N. Pourmohammadi Vafa, Microstructure and mechanical properties of Ti₃SiC₂ MAX phases sintered by hot pressing, *Synth. Sinter.* 1 (2021) 216–222. <https://doi.org/10.53063/synsint.2021.1472>.
- [18] C.-h. Yang, F. Wang, T.-t. Ai, J.-f. Zhu, Microstructure and mechanical properties of in situ TiAl/Ti₂AlC composites prepared by reactive hot pressing, *Ceram. Int.* 40 (2014) 8165–8171. <https://doi.org/10.1016/j.ceramint.2014.01.012>.
- [19] B. Mei, Y. Miyamoto, Investigation of TiAl/Ti₂AlC composites prepared by spark plasma sintering, *Mater. Chem. Phys.* 75 (2002) 291–295. [https://doi.org/10.1016/S0254-0584\(02\)00078-0](https://doi.org/10.1016/S0254-0584(02)00078-0).
- [20] F. Yang, F.T. Kong, Y.Y. Chen, S.L. Xiao, Effect of spark plasma sintering temperature on the microstructure and mechanical properties of a Ti₂AlC/TiAl composite, *J. Alloys Compd.* 496 (2010) 462–466. <https://doi.org/10.1016/j.jallcom.2010.02.077>.
- [21] T.A. Otitoju, P.U. Okoye, G. Chen, Y. Li, M.O. Okoye, S. Li, Advanced ceramic components: Materials, fabrication, and applications, *J. Ind. Eng. Chem.* 85 (2020) 34–65. <https://doi.org/10.1016/j.jiec.2020.02.002>.
- [22] J. Venezuela, M.S. Dargusch, The influence of alloying and fabrication techniques on the mechanical properties, biodegradability and biocompatibility of zinc: A comprehensive review, *Acta Biomater.* 87 (2019) 1–40. <https://doi.org/10.1016/j.actbio.2019.01.035>.
- [23] N.F. Mogale, W.R. Matizamhuka, Spark Plasma Sintering of Titanium Aluminides: A Progress Review on Processing, Structure-Property Relations, Alloy Development and Challenges, *Metals (Basel).* 10 (2020) 1080. <https://doi.org/10.3390/met10081080>.
- [24] L. Čelko, M. Menelaou, M. Casas-Luna, M. Horynová, T. Musálek, et al., Spark Plasma Extrusion and the Thermal Barrier Concept, *Metall. Mater. Trans. B.* 50 (2019) 656–665. <https://doi.org/10.1007/s11663-018-1493-3>.
- [25] M. Akhlaghi, E. Salahi, S.A. Tayebifard, G. Schmidt, Role of Ti₃AlC₂ MAX phase on characteristics of in-situ synthesized TiAl intermetallics. Part I: sintering and densification, *Synth. Sinter.* 1 (2021) 169–175. <https://doi.org/10.53063/synsint.2021.1347>.
- [26] M. Akhlaghi, E. Salahi, S.A. Tayebifard, G. Schmidt, Role of Ti₃AlC₂ MAX phase on characteristics of in-situ synthesized TiAl intermetallics. Part II: Phase evolution, *Synth. Sinter.* 1 (2021) 211–216. <https://doi.org/10.53063/synsint.2021.1453>.
- [27] M. Akhlaghi, E. Salahi, S.A. Tayebifard, G. Schmidt, Role of Ti₃AlC₂ MAX phase on characteristics of in-situ synthesized TiAl intermetallics. Part III: microstructure, *Synth. Sinter.* 2 (2022) 20–25. <https://doi.org/10.53063/synsint.2022.2182>.
- [28] M. Akhlaghi, S.A. Tayebifard, E. Salahi, M. Shahedi Asl, G. Schmidt, Self-propagating high-temperature synthesis of Ti₃AlC₂ MAX phase from mechanically-activated Ti/Al/graphite powder mixture, *Ceram. Int.* 44 (2018) 9671–9678. <https://doi.org/10.1016/j.ceramint.2018.02.195>.
- [29] Y. Liu, W. Zhang, Y. Peng, G. Fan, B. Liu, Effects of TiAl Alloy as a Binder on Cubic Boron Nitride Composites, *Materials (Basel).* 14 (2021) 6335. <https://doi.org/10.3390/ma14216335>.
- [30] L. Rangaraj, V. Kashimatt, Pooja, B. Suresha, Reaction, densification and mechanical properties of Ti₂AlC_x ceramics at low applied pressure and temperature, *Int. J. Appl. Ceram. Technol.* (2022). <https://doi.org/10.1111/ijac.14064>.
- [31] J. Wang, N. Zhao, P. Nash, E. Liu, C. He, et al., In situ synthesis of Ti₂AlC-Al₂O₃/TiAl composite by vacuum sintering mechanically alloyed TiAl powder coated with CNTs, *J. Alloys Compd.* 578 (2013) 481–487. <https://doi.org/10.1016/j.jallcom.2013.06.109>.
- [32] M. Liu, J. Chen, H. Cui, X. Sun, S. Liu, M. Xie, Ag/Ti₃AlC₂ composites with high hardness, high strength and high conductivity, *Mater. Lett.* 213 (2018) 269–273. <https://doi.org/10.1016/j.matlet.2017.11.038>.
- [33] Y. Wang, M. Yao, Z. Hu, H. Li, J.-H. Ouyang, et al., Microstructure and mechanical properties of TiB₂-40 wt% TiC composites: Effects of adding a low-temperature hold prior to sintering at high temperatures, *Ceram. Int.* 44 (2018) 23297–23300. <https://doi.org/10.1016/j.ceramint.2018.09.048>.
- [34] C.L. Yeh, C.Y. Ke, Y.C. Chen, In situ formation of TiB₂/TiC and TiB₂/TiN reinforced NiAl by self-propagating combustion synthesis, *Vacuum.* 151 (2018) 185–188. <https://doi.org/10.1016/j.vacuum.2018.02.024>.
- [35] Z. Aygüzer Yaşar, A.M. Celik, R.A. Haber, Improving fracture toughness of B₄C-SiC composites by TiB₂ addition, *Int. J. Refract. Met. Hard Mater.* 108 (2022) 105930. <https://doi.org/10.1016/j.ijrmhm.2022.105930>.
- [36] Y. Liu, Z. Li, Y. Peng, Y. Huang, Z. Huang, D. Zhang, Effect of sintering temperature and TiB₂ content on the grain size of B₄C-TiB₂ composites, *Mater. Today Commun.* 23 (2020) 100875. <https://doi.org/10.1016/j.mtcomm.2019.100875>.